1,25(OH)$_2$vitamin D$_3$ inhibits cell proliferation by promoting cell cycle arrest without inducing apoptosis and modifies cell morphology of mesenchymal multipotent cells

Jorge N. Artaza [a,b,*], Fara Sirad [a], Monica G. Ferrini [a,b], Keith C. Norris [a,b]

[a] Department of Internal Medicine, Charles Drew University of Medicine & Science, Los Angeles, CA 90059, USA
[b] Department of Medicine, David Geffen School of Medicine at UCLA, Los Angeles, CA 90095, USA

ARTICLE INFO

ABSTRACT

The vitamin D receptor (VDR) and its ligand 1,25D play an important role in regulating cell growth and cell fate. We examined the effect of 1,25D on cell morphology, cell proliferation, cell cycle progression and apoptosis on mesenchymal multipotent cells. Multipotent cells were treated with and without 1,25D in a time- and dose-dependent manner. Changes in cell morphology were evaluated by a green fluorescence fluorocrome. Cell proliferation was determined by the Formazan assay and PCNA antigen expression. The expression of genes related to the cell cycle was analyzed by DNA microarrays, RT^{2}PCR arrays and western blots. Apoptosis was evaluated by TUNEL assay, and the expression of pro- and anti-apoptotic related genes by RT^{2}PCR arrays and western blots. 1,25D inhibited cell proliferation, induced cell cycle arrest, and promoted accumulation of cells in G0/G1 phase without inducing apoptosis. An increase in cell size was associated with a decrease in the GTPase Rho and the atypical Rho family GTPase Rhou/Wrch-1 expression without inducing Wnt-1 expression. Survivin expression was also increased and may represent a novel 1,25D-mediated pathway regulating tissue injury and fibrosis. The data provide a mechanistic explanation for the anti-proliferative and anti-apoptotic properties of 1,25D in mesenchymal multipotent cells.

© 2010 Elsevier Ltd. All rights reserved.

1. Introduction

Vitamin D, a fat-soluble pro-hormone, is obtained from dietary sources or from *de novo* synthesis in the skin as a result of ultraviolet light-induced photolytic conversion of 7-dehydrocholesterol to previtamin D3, followed by thermal isomerization to vitamin D3 [1,2]. The first step in the metabolic activation of vitamin D is the hydroxylation of carbon 25 (25OHD), which occurs primarily in the liver. The second and more regulated step in vitamin D bioactivation is the formation of 1α,25-dihydroxyvitamin D$_3$ (1,25D), also known as calcitriol, which occurs mainly in the kidney [3] via the 25OHD-1α-hydroxylase enzyme, although numerous cells and tissues express 1α-hydroxylase [4]. 1,25D binds to the vitamin D receptor (VDR), a nuclear receptor and a member of the steroid/thyroid hormone superfamily receptors, which acts as a ligand-activated transcription factor [5]. VDR functions as a heterodimer with retinoid X receptor; upon ligand binding, VDR undergoes a conformational change that promotes retinoid X receptor–VDR heterodimerization [6]. The binded heterodimer translocates to the nucleus, where VDR binds to the vitamin D response elements, induces chromatin-modifying enzymatic activities, and ultimately modulates gene transcription [7]. The VDR appears to be ubiquitous, supporting the vitamin D endocrine system's involvement in a wide range of physiological functions [8–11].

It has been extensively reported that 1,25D can, in general, inhibit the growth of normal and malignant cell types. Previous studies on the mechanism behind this growth-inhibitory action have revealed that 1,25D-induced inhibition of cell growth is probably mediated via different combinations of pathways and mechanisms in varying cell types [12]. In view of its potent anti-proliferative and prodifferentiating action, and the presence of the VDR in a large variety of cells, 1,25D or select analogs could be considered a promising intervention to prevent and treat hyperproliferative disorders [11,12]. Elucidation of the molecular mechanism underlying cell cycle related anti-proliferative action of 1,25D could help identify new biomarkers for increased disease-specific risk in vitamin D-deficient persons as well as targeting treatments with novel vitamin D analogs.

Studies of the effects of calcitriol on apoptosis are contradictory and depend mostly on the cell model applied. It has been reported that 1,25D induced apoptosis in peripheral blood mononuclear cell (PBMC) obtained from healthy subjects and in inflammatory bowel disease (IBD) patients [13]. By contrast, other studies have reported an inhibitory effect of calcitriol on hepatocyte apoptosis in rat allograft by upregulating anti-apoptosis-associated genes [14]. Concerning the effects of 1,25D on cell morphology/phenotype, it has been reported that 1,25D profoundly affects the phenotype of breast cancer cells, suggesting that it reverts the myoepithelial features associated with more aggressive forms and poor prognosis in human breast cancer, increasing cell and nuclear size, and inducing a change from a rounded to a flattened morphology [15]. C3H 10T1/2 is a well-known and widely used mesenchymal multipotent cell line *in vitro* model that has been shown by us and others to have the potential to differentiate into a variety of specialized cells such as osteocytes, chondrocytes, adipocytes, endothelial and smooth muscle cells (SMCs) [16–23] and they have been used as a cell model to study the effects of myostatin [24] and 1,25D on fibrosis [20] and cytokinesis [23]. C3H 10T1/2 cells are also considered an important model to systematically identify and analyze specific gene products that play an early role in cell proliferation and cell fate [20,26]. Moreover, there are no reports in the literature assessing the effects of 1,25D on apoptosis, cell morphology/phenotype in C3H 10T1/2 mesenchymal multipotent cells.

In this study all C3H 10T1/2 mesenchymal multipotent cells were primed with 5′-azacytidine [17,19,20,24,25,26,28] allowing us to evaluate the independent effects of 1,25D in comparison to no 1,25D at an early stage when cells still have the ability to undergo differentiation [19,20]. C3H 10T1/2 cells have the ability to differentiate into multiple cell lineages according to the cell culture conditions such as incubation medium, cell density, and/or the addition of factors such as androgens [17,28] or TGFβ factors [19,24]. This is in contrast to progenitor cells that are already committed to a single cell lineage or terminally differentiated cells [27,29–31]. This approach allowed us to explore potential novel 1,25D-mediated pathways that could provide the foundation for future adjuvant therapeutic approaches to address select hypovitaminosis D related chronic disease states.

Given the rapid advances in regenerative medicine such as the promise of induced pluripotent stem cells, a better understanding of 1,25D in mesenchymal multipotent cells is poised to accelerate the translation of novel basic science findings into human clinical trials. Thus, the aim of the present study was to provide evidence of the molecular mechanism (s) by which 1,25D affects cell morphology, cell proliferation, cell cycle progression and apoptosis using a well-known and widely used mesenchymal multipotent cell line.

2. Materials and methods

2.1. Cell culture

Mouse C3H 10T1/2 multipotent mesenchymal cells (MMCs) (ATCC, Manassas, VA, USA) grown in DMEM supplemented with 10% dialyzed fetal bovine serum at 37 °C and 5% CO_2 were treated with 20 μM 5′-azacytidine (AZCT) for 2 days to induce differentiation by epigenetic changes [16,17,19,20]. Cells were split in a 1:2 ratio, allowed to recover for 2 days, and replated at 60–70% confluence in T75 flasks, 8-well chamber slides or 6-well plates. The next day, cells were incubated with and without 100 nM of 1,25D (Sigma–Aldrich, St. Louis, MO, USA) dissolved in less than 0.1% ethanol as vehicle in DMEM 10% dialyzed fetal bovine serum for 4 and 7 days. For proliferation studies, mesenchymal multipotent cells primed with AZCT were incubated with 1,25D (10–500 nM) for 4 days, in the same way control groups were incubated with

0.1% ethanol in DMEM 10% dialyzed fetal bovine serum (Invitrogen, Carlsbad, CA, USA). Because of the short half-life of 1,25D, the cell culture media with and without 1,25D (10–500 nM) was replaced every 24 h.

2.2. Cell proliferation assay

Cell proliferation was determined in 96-well plates by the Formazan dye assay (Promega Corp., Madison, WI, USA). Cells were grown at an initial density of 4000 cells/well; and then treated for 4 days with 1,25D in a concentration range from 10 to 500 nM. At the end of the incubation time, 100 μl of Formazan substrate buffer was added to the cultures for 3 h at 37 °C in 5% CO_2, and the absorbance at 490 nm was read. For cell counting, cells were removed by trypsinization and the number of viable cells was counted in a hemocytometer with the use of Trypan blue staining [32].

Cell proliferation was also evaluated/confirmed by changes in gene expression of a related cell proliferation antigen after 4 days incubation time with or without 1,25D. The cell proliferation antigen applied was the proliferating cell nuclear antigen (PCNA) a protein essential for DNA replication, repair and cell proliferation [33].

2.3. Cell morphology/phenotype

Changes in cell morphology/phenotype were determined in living cells in culture by the PKH2 Green Fluorescent Cell Linker assay (Sigma–Aldrich, Saint Louis, MO, USA) [34]. After an initial and stable incorporation of the PKH2-GL (2×10^{-6} M) into the lipid regions of the cell membrane, cells were counterstained with DAPI 0.02% (Invitrogen, Carlsbad, CA, USA). Cells were grown at an initial density of 8000 cells/well in 8-well chamber slides and were treated for 4 and 7 days, respectively, with or without 1,25D (100 nM). Serial pictures were taken every 24 h with a fluorescent microscope equipped with green and blue filters. The serial pictures at 200× and 400× magnification were taken with a Leica DMLB fluorescence microscope coupled to Spot RT digital camera.

The area and the number of cells per field were analyzed using ImagePro-Plus 5.1 software (Media Cybernetics, Silver Spring, MD, USA). At least 10 pictures were taken per treatment group per well done in duplicate. The experiments were repeated at least three times.

2.4. Apoptosis

The apoptotic index was determined by the TdT-mediated dUTP nick end labeling (TUNEL) method, based on the ability of terminal TdT to catalyze addition of digoxenin-dUTP and dATP to 3′-OH ends of cleaved DNA. Cells were seeded on 8-well chamber slides and were incubated with or without 1,25D (100 nM) for 4 days and then fixed in 2% p-formaldehyde in 1× PBS. Cells were treated with 2% H_2O_2 for quenching endogenous peroxidase activity, digoxigenin-conjugated nucleotides and TdT, and finally anti-digoxigenin-peroxidase. Sections were stained with 0.5% diaminobenzidine/0.01% H_2O_2, and counterstained with hematoxylin. As a negative control, PBS (1×) buffer was substituted for the TdT enzyme. Quantification of the apoptotic index was done at 400×. In all cases, 20 fields were randomly selected and the apoptotic index of each field was calculated as the percent of TUNEL-positive cells [32].

2.5. DNA microarray analysis of cell cycle target genes

Total cellular RNA was isolated with Trizol-Reagent (Invitrogen, Carlsbad, CA, USA) from C3H 10T1/2 cells undergoing differen-

tiation with 5′-azacytidine (AZCT), and treated with or without 1,25D (100 nM) for 4 days. Isolated RNA was subjected to cDNA gene arrays (Oligo GEArray, Cell Cycle gene array (OMM-020) SABiosciences Corp., Frederick, MD, USA). The Mouse Cell Cycle Microarray profiles the expression of 112 genes key to cell cycle regulation such as CDKs and CDK-modifying proteins, including cyclins, CDK inhibitors, CDK phosphatases, and CDK kinases, as well as genes in the APC ubiquitin–conjugation complexes. Biotin-labeled cDNA probes were synthesized from total RNA, denatured, and hybridized overnight at 60 °C in GE Hybridization solution to membranes spotted with cell cycle related genes. Membranes were washed, and chemiluminescent analysis was performed as per the manufacturer's instructions. Raw data were analyzed using GE Array Expression Analysis Suite (SABiosciences Corp., Frederick, MD). Fold changes in relative gene expression were presented after background correction and normalization with a housekeeping gene [24,35].

2.6. RT^2 Profiler^{TM} PCR array analysis of cell cycle and apoptosis target genes

RT^2 Profiler^{TM} PCR SABiosciences analysis of cell cycle and apoptosis target genes were applied in triplicates in order to confirm the GE Array data (cell cycle) and to complement the TUNEL and western blot results (apoptosis). Aliquots of total cellular RNA isolated with Trizol-Reagent from C3H 10T1/2 cells undergoing differentiation with 5′-azacytidine (AZCT) were treated with or without 1,25D (100 nM) for 4 days. They were then subjected to reverse transcription, and the resulting cDNA was analyzed by: RT^2 Profiler^{TM} PCR Mouse Cell Cycle Array (PAMM-020) and by RT^2 Profiler PCR mouse apoptosis (PAMM-012) (SABiosciences Corp., Frederick, MD, USA). The Mouse Cell Cycle RT^2 Profiler^{TM} PCR Array profiles the expression of genes that both positively and negative regulate the cell cycle, the transitions between each of the phases, DNA replication, checkpoints and arrest. The Mouse Apoptosis RT^2 Profiler^{TM} PCR Array profiles the expression of genes involved in apoptosis, or programmed cell death. Each array contains a panel of 84 primer sets related to the cell cycle and to apoptosis plus 5 housekeeping genes and 2 negative controls. Real-time PCRs were performed as follows: melting for 10 min at 95 °C, 40 cycles of two-step PCR including melting for 15 s at 95 °C, annealing for 1 min at 60 °C. The raw data were analyzed using the $\Delta\Delta C_t$ method following the manufacturer's instructions (SABiosciences Corp., Frederick, MD, USA) [24,35].

2.7. Real-time quantitative PCR

Total RNA was extracted using Trizol-Reagent (Invitrogen, Carlsbad, CA) and equal amounts (1 μg) of RNA were reverse transcribed using a RNA PCR kit (Applied Biosystems, Foster City, CA, USA). Mouse gene PCR primer sets (RT^2) for PCNA, Casp3, Wrch-1 and Wnt-1 were obtained from SuperArray Bioscience (SABiosciences Corp., Frederick, MD, USA). The QIAGEN Sybr Green PCR kit with HotStar Taq DNA polymerase (QIAGEN, Valencia, CA, USA) was used with i-Cycler PCR thermocycler and fluorescent detector lid (Bio-Rad, Hercules, CA, USA) [35].

The protocol included melting for 15 min at 95 °C, 40 cycles of three-step PCR including melting for 15 s at 95 °C, annealing for 30 s at 58 °C, elongation for 30 s at 72 °C with an additional detection step of 15 s at 81 °C, followed by a melting curve from 55 to 95 °C at the rate of 0.5 °C per 10 s. Samples of 25 ng cDNA were analyzed in quadruplicate in parallel with GAPDH controls; standard curves (threshold cycle vs. log pg cDNA) were generated by log dilutions of from 0.1 pg to 100 ng standard cDNA (reverse-transcribed mRNA from C3H 10T1/2 cells in AM). Experimental mRNA starting quantities were then calculated from the standard curves and aver-

aged using i-Cycler, iQ software as described previously [20]. The ratios of marker experimental gene (e.g. PCNA, Casp3 and Wrch-1 mRNA) to GAPDH mRNA were computed and normalized to control (untreated) samples as 100%.

2.8. Immunocytochemical analyses of PCNA antigen

After incubating the MMCs for 4 days with and without 1,25D, cells were washed five times with PBS (1×) and fixed by immersion in 2% p-formaldehyde, quenched with H_2O_2, blocked with normal horse serum and incubated with anti-proliferating cell nuclear antigen (PCNA) monoclonal antibody (1:400) (Millipore, Temecula, CA, USA). Detection was based on a secondary biotinylated antibody (1:200), followed by the addition of the streptavidin–horseradish peroxidase ABC complex (1:100), Vectastain (Elite ABC System, Vector Laboratories, Burlingame, CA, USA) and 3,3′-diaminobenzidine and H_2O_2 mixture (Sigma, St. Louis, MO). The MMCs were counterstained with Mayer's hematoxylin solution (Sigma–Aldrich, St. Louis, MO, USA). In negative controls, we either omitted the first antibody or used a rabbit non-specific IgG.

2.9. Western blot and densitometric analysis

Cell lysates (25–40 μg of protein) were subjected to western blot analyses by 4–15% Tris–HCl polyacrylamide gel electrophoresis (PAGE) (Bio-Rad, Hercules, CA, USA) in running buffer (Tris/Glycine/SDS). Proteins were transferred overnight at 4 °C to nitrocellulose membranes in transfer buffer (Tris/Glycine/Methanol). Next day, the non-specific binding was blocked by immersing the membranes into 5% non-fat dried milk, 0.1% (v/v) Tween 20 in PBS for 2 h at room temperature. After several washes with washing buffer (PBS Tween 0.1%), membranes were incubated with the primary antibodies for 3 h at room temperature or overnight at 4 °C, monoclonal antibodies were as follows: (a) PCNA (1/500) (Millipore, Temecula, CA, USA), (b) glyceraldehyde-3-phosphate dehydrogenase (GAPDH) (1/10,000) (Chemicon International, Temecula, CA, USA), (c) Bcl-2 (1/500) (BD Biosciences, San Jose, CA, USA), (d) Cyclin D1 (1/500), (e) Cyclin D3 (1/500), and (f) Cdk4 (1/500) (Cell Signaling Technology, Inc., Danvers, MA, USA) and Rho (1/500) (Abcam Inc., Cambridge, MA, USA). Polyclonal antibodies were used for (a) Cdk2 (1/500), (b) p21 (1/500) and (c) p27 (1/500) (Santa Cruz Biotechnology, Inc., Santa Cruz, CA, USA). The washed membranes were incubated for 1 h at room temperature with 1/3000 dilution (anti-mouse) or 1:2000 dilution (anti-rabbit) of secondary antibody linked to horseradish peroxidase, respectively (Cell Signaling Technology, Inc., Danvers, MA, USA). After several washes, the immunoreactive bands were visualized using the SuperSignal western blotting chemiluminescence detection system (Thermo Fisher Scientific, Inc., Rockford, IL, USA). The densitometric analysis of the bands was done with the Scion Image software beta 4.02 (Scion Corp., Frederick, MD, USA).

2.10. Qualitative and quantitative immunocytochemical analyses

The immunoreactivity was quantified by Image Analysis using ImagePro-Plus 5.1 software (Media Cybernetics, Silver Spring, MD, USA). Fields are counted blindly by two independent observers and each experiment was repeated three times. For PCNA and TUNEL determinations, the number of positive cells at 400× was counted in a computerized grid and results were expressed as a % of positive cells/total cells per field. In all cases, 8 fields at 400× were analyzed per wells.

Cell size was determined by outlining and measuring the area of each cell per field. Approximately 100 cells were measured for

each experiment and the results were converted in cell size histograms plotting the number of cells per area expressed in μm^2. To test the precision of the QIA, we evaluated both inter- and intra-assay variability. Standard deviation was 0.39 for assays in triplicate, CV = 1.9% for intra-assay determinations and CV 4.0% for inter-assay.

The results expressed as mean ± SEM represent the average of three independent experiments [19,20,24].

2.11. Statistical analysis

All data are presented as mean ± SEM, and between-group differences were analyzed using ANOVA. If the overall ANOVA revealed significant differences, then pair-wise comparisons between groups were performed by Tukey's multiple comparison test. All comparisons were two-tailed, and p values less than 0.05 were considered statistically significant. The in vitro experiments were repeated thrice, and data from representative experiments are shown. Specifically, the DNA microarray tests were done twice and the results confirmed by RT^2 Profiler^{TM} PCR arrays in triplicates and in some cases by qRT-PCR in triplicates.

3. Results

3.1. 1,25D inhibits cell proliferation of C3H 10T1/2 mesenchymal multipotent cells

Even though we seeded the same number of cells, incubation with 1,25D (100 nM) for 4 days shows a noticeable decrease in cell number per field compared to control cells (no 1,25D) (Fig. 1A). To assess whether 1,25D inhibits C3H 10T1/2 multipotent cell replication, an initial number of 4000 cells/well (low confluence) were seeded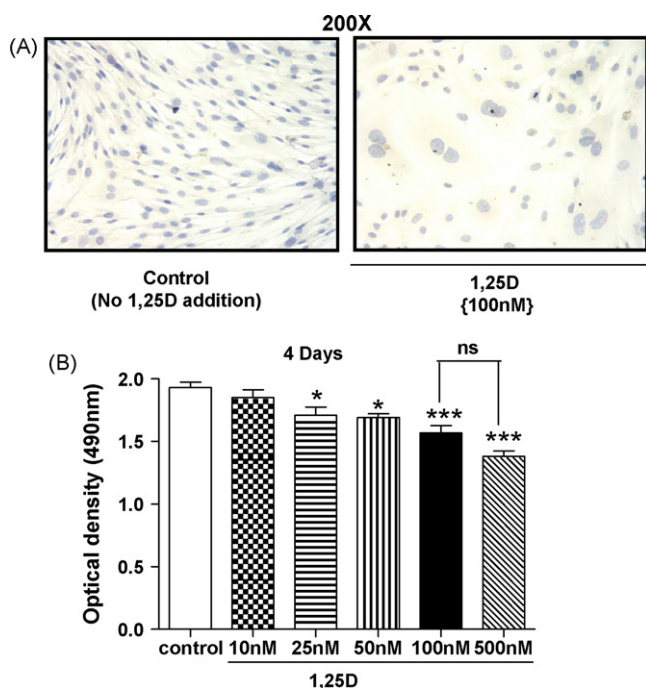 in 96-well plates and incubated in triplicates with increasing concentrations of 1,25D, from 10 to 500 nM, for 4 days, and at the end of the incubation time, cell proliferation was evaluated by the Formazan assay (Fig. 1B). Starting at 25 nM, 1,25D induced a statistically significant reduction in cell number reaching a plateau at 100 nM. For that reason, 100 nM was the dose applied throughout the study to evaluate the effects of 1,25D on mesenchymal multipotent cells.

In order to confirm the anti-proliferative effect of 1,25D on mesenchymal multipotent cells, PCNA expression was evaluated. Incubation of cells with 1,25D decreased the expression of proliferating cell nuclear antigen (PCNA) as assessed by several approaches; Fig. 2A, left panel shows representative pictures at 200× and 400× magnification of the decreased expression of PCNA upon incubation with 1,25D (100 nM) for 4 days by immunocytochemistry (ICC). The visual inspection was confirmed by quantitative image analysis (Fig. 2A, right panel) where PCNA expression was significantly decreased by 3-fold with respect to the control ($p < 0.001$). The decreased expression of PCNA was further confirmed by real-time PCR (PCNA/GAPDH ratio: −2.05) (Fig. 2B) and by western blot (Fig. 2C, left) with the corresponding densitometric analysis (Fig. 2C, right).

3.2. 1,25D modifies cell morphology increasing cell size of C3H 10T1/2 mesenchymal multipotent cells

In order to verify our previous visual observations regarding changes in cell number and size upon incubation of multipotent cells with 1,25D, cells were pre-labeled with a cell membrane marker, the PKH2 Green Fluorescent Cell Linker and DAPI to visualize cell boundaries and cell nuclei respectively and later incubated with or without 1,25D for 4 and 7 days. Four days incubation with 1,25D significantly increased the morphology/phenotype/size and decreased cell number of mesenchymal multipotent cells (Fig. 3A, upper panel). The visual inspection was further confirmed by QIA (quantitative image analysis) shown in Fig. 3A, lower panel where the histogram shows a shift from smaller cells to larger cells in the population indicating that 1,25D significantly increased cell size and reduce cell number per field with respect to the control. Similar results were obtained in a parallel experiment where cells were incubated for 7 days. Representative pictures can be observed in Fig. 3B, upper panel and the corresponding QIA (quantitative image analysis) Fig. 3B, lower panel. Incubation of mesenchymal multipotent cells with 1,25D (100 nM) for 7 days increased cell size, modified cell morphology and reduced cell number per field.

3.3. Addition of 1,25D downregulate the expression of Rho a member of the Ras superfamily of low molecular weight GTPases and the atypical GTPase Rhou/Wrch-1 without increasing Wnt-1 expression in C3H 10T1/2 mesenchymal multipotent cells

In order to clarify the mechanism by which 1,25D changes cell morphology, the expression of a novel gene Wrch-1 involved in regulating cell morphology, cytoskeletal organization, and cell proliferation was evaluated. We found that upon incubation with 1,25D (100 nM) for 4 days the mRNA levels of Rhou/Wrch-1 were decreased by 4.5-fold as determined by real-time PCR (qRT-PCR) compared to control (no 1,25D addition) (Fig. 4A, upper panel). In addition, Fig. 4, panel B left shows decreased expression upon 1,25D incubation for 4 days of Rho, a member of the GTPase family which has been linked to biological pathways related to cytoskeletal dynamics, polarity, cell survival/apoptosis and cell proliferation, by western blot with the corresponding densitometric analysis (Fig. 4, panel B right).

Fig. 4, panel C, shows no changes in mRNA expression of Wnt-1 by real-time PCR (qRT-PCR) after addition of 1,25D (100 nM) for 4 days, demonstrating no activation of Wnt-1 signaling by 1,25D.
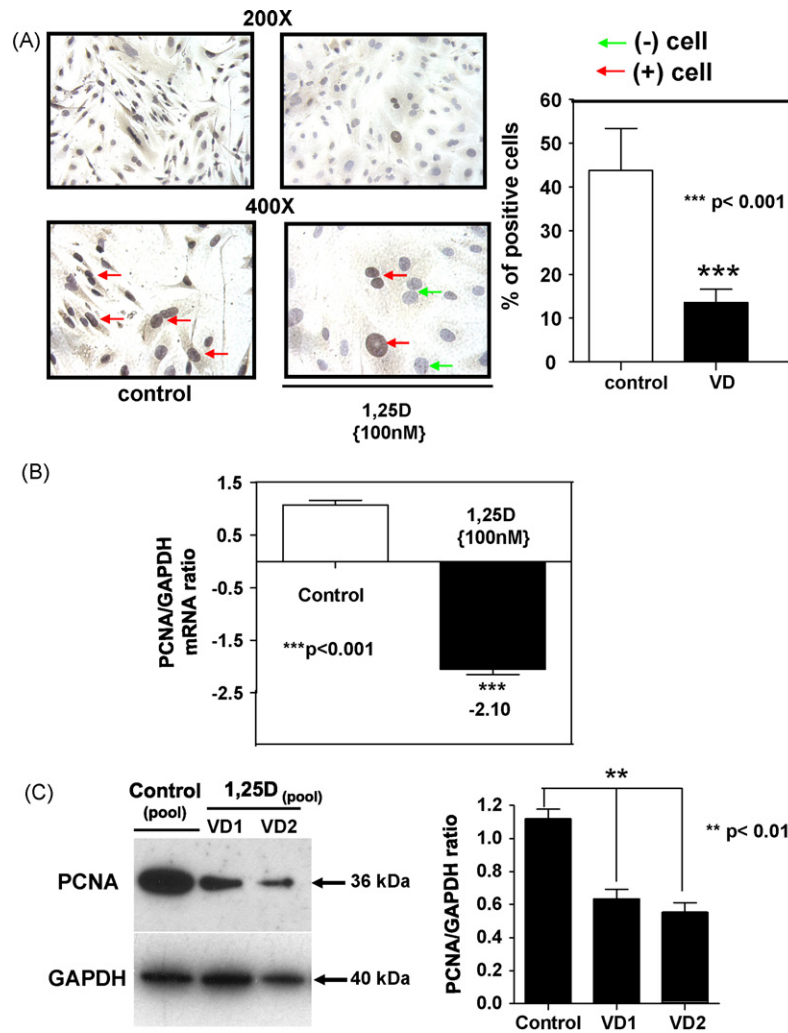

Fig. 1. 1,25D inhibits cell proliferation in multipotent mesenchymal C3H 10T1/2 in a dose-dependent manner. (A) Cells treated with or without 1,25D (100 nM) for 4 days were fixed with 2% p-formaldehyde and counterstained with hematoxylin (200×). (B) C3H 10T1/2 cells primed with 5′-azacytidine (20 μM) at an initial number of 4000 cells/well were incubated for 4 days, as follows: control: no addition of 1,25D and 1,25D: increasing concentrations of 1,25D from 10 to 500 nM. Results are expressed as mean ± SEM. *$p < 0.05$; ***$p < 0.001$.

Fig. 2. 1,25D downregulates the expression of proliferating cell nuclear antigen (PCNA). Cells treated as in Fig. 1 were incubated with or without 100 nM of 1,25D for 4 days. Immunocytochemistry for PCNA were performed at the end of the incubation time (A). Mean ± SEM corresponds to experiments done in triplicates of the percentage of positive cells (brown nuclear staining) by quantitative image analysis. ***$p < 0.001$. (B) Total RNA isolation followed by real-time PCR was applied in other aliquots for the 4 days incubation normalized by GAPDH housekeeping gene. Mean ± SEM corresponds to experiments done in triplicates ***$p < 0.001$. (C) Western blots analysis was performed for extracts from the 4 days incubation time (left) and the corresponding densitometric analysis (right) 200× and 400×.

3.4. 1,25D exerts an anti-apoptotic effect in C3H 10T1/2 mesenchymal multipotent cells

To investigate whether 1,25D might control cell number through the regulation of programmed cell death, we incubated the cells with 1,25D (100 nM) for 4 days and assessed selected apoptotic markers by different approaches. Fig. 5 shows there was no significant effect of 1,25D on the number of apoptotic cells determined by TUNEL assay (Fig. 5A, left) followed by quantitative image analysis (Fig. 5A, right). In contrast, Fig. 5B shows that incubation of multipotent cells with 1,25D (100 nM) for 4 days exerts an anti-apoptotic effect decreasing the expression of pro-apoptotic genes such as caspase 3 by 2.12-fold ($p < 0.001$) as assessed by real-time PCR. Moreover, the addition of 1,25D (100 nM) to the cell culture promotes the upregulation of anti-apoptotic markers such as Bcl-2 evaluated by western blot (Fig. 5C, left) with corresponding densitometric analysis (Fig. 5C, right) and confirmed by RT² PCR arrays (Table 1 Bcl-2 (+2.9)).

The anti-apoptotic effects of 1,25D on C3H 10T1/2 were further analyzed at the transcriptional level by applying the RT² Profiler™ real-time apoptosis PCR array (PAMM-012). Table 1 shows the ratios of determinations done in triplicate after continuous incubation with and without 1,25D for 4 days. Table 1

shows that C3H 10T1/2 cells incubated with 1,25D (100 nM) for 4 days increased the total mRNA expression of Apoptosis Inhibitor-5/anti-apoptosis clone 11 (Api5/Aac11) (+2.16), which is a critical determinant of dE2F1-induced apoptosis *in vivo* and *in vitro*. Table 1 shows also an increased expression of Bcl-2 (+2.9)

Table 1

1,25D modulates the transcriptional expression of apoptosis-related genes in C3H 10T1/2 multipotent mesenchymal cells Total RNA from cells treated as in Fig. 2 was subjected to RT-real-time PCR by the Mouse Apoptosis RT² Profiler™ PCR Array and the ratios between the 1,25D-treated and 1,25D-untreated cells corrected by GAPDH were calculated for the assays performed in triplicates.

| Symbol	Description	Real-time PCR array ratios (4 days)
Api5/Aac11	Apoptosis inhibitor 5	+2.16
Atf5	Activated transcription factor 5	−2.81
Bcl-2	B-cell leukemia/lymphoma 2	+2.9
Birc5	Baculoviral IAP repeat-containing 5 (survivin)	+4.53
Casp3	Caspase 3	−2.30
BAX	Bcl-2-associated X protein	1.18
BAD	Bcl-2-associated death promoter	1.22
BAK	BCL-2-antagonist/killer	1.36
BOK	Bcl-2-related ovarian killer protein	1.29
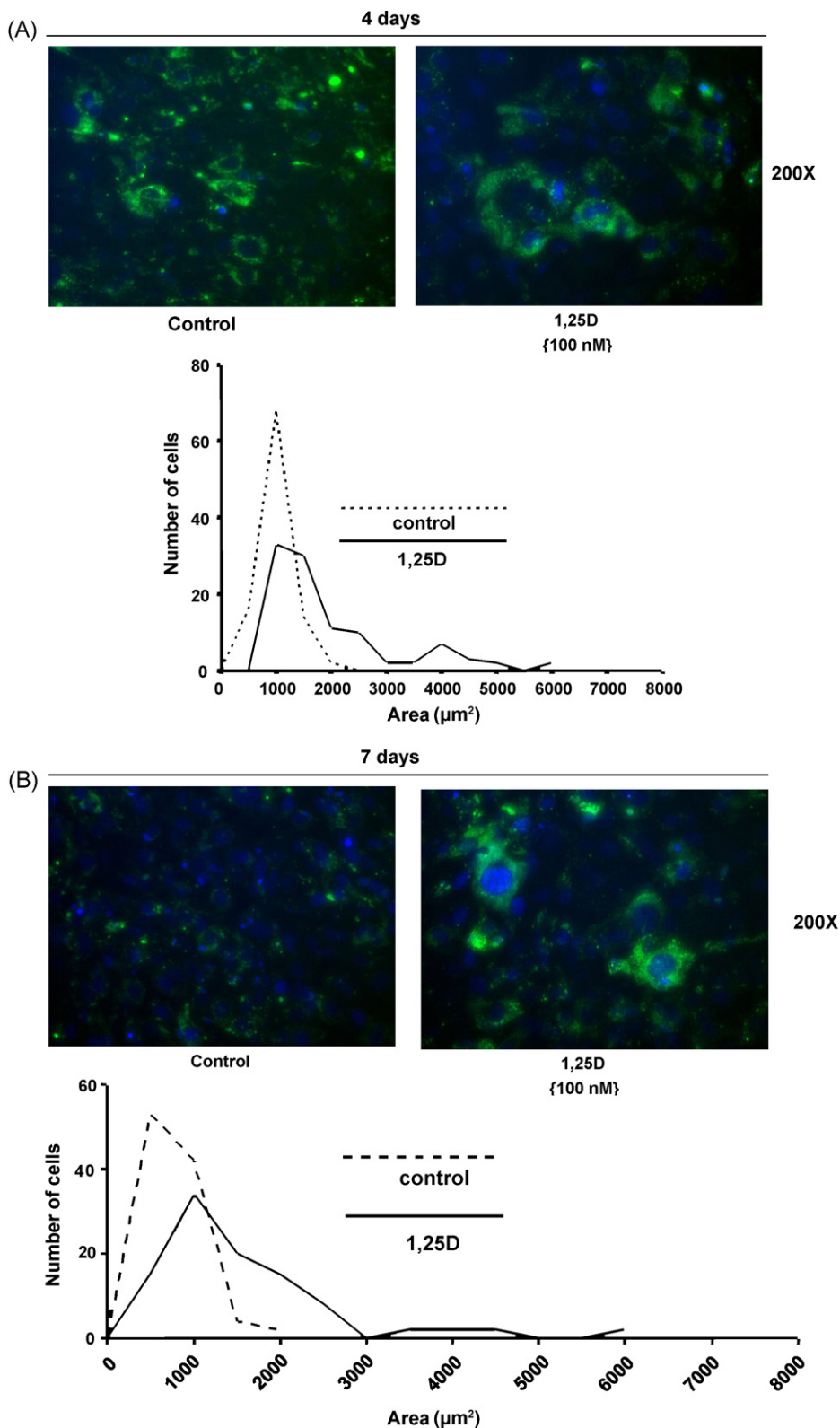
Fig. 3. 1,25D decreases cell number and increases cell size of multipotent mesenchymal cells. Cells treated as in Fig. 1 were preincubated with Green Fluorescent Cell Linker (PKH2) and counterstaining with DAPI. Next day, cells were incubating with or without 1,25D for 4 and 7 days, respectively. Representative pictures are presented for control (no 1,25D addition) and 1,25D (100 nM) at 4 days (A upper panel) and at 7 days (B, upper panel) with the corresponding histograms showing the cell size distribution and expressing the number of cells per area (μm^2) (A and B, lower panels).

in agreement with the western blot shown in Fig. 5; and Baculoviral IAP repeat-containing 5 (Birc5) (+4.53) also known as "survivin", a protein that inhibits apoptosis and regulates cell division.

In addition, incubation of multipotent mesenchymal cells with 1,25D (100 nM) decreases the expression of select pro-apoptotic genes such as activated transcription factor 5 (Atf5) (−2.81), which plays an essential role in hematopoietic and glioma cell survival and
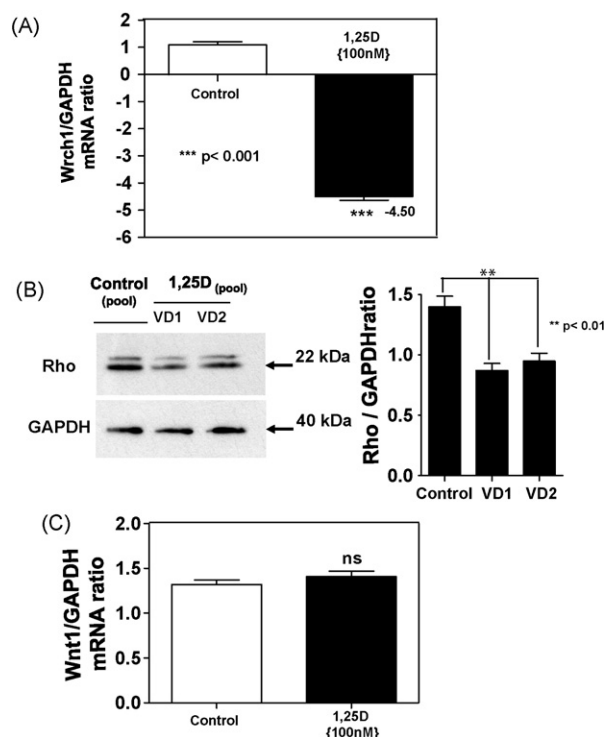
Fig. 4. 1,25D regulates cell size through downregulation of the GTPase Rho and the atypical rho family GTPase Rhou/Wrch-1 without intervention of Wnt-1. Total RNA isolation from cells treated as in Fig. 2, was subjected to real-time PCR for Wrch-1 normalized by GAPDH housekeeping gene (A). Mean ± SEM corresponds to experiments done in triplicates ***$p < 0.001$. (B) Western blot analysis was performed for extracts from the 4 days incubation time for Rho normalized with GAPDH with the correspondent densitometric analysis. In another set of aliquots the RNA samples were utilized for real-time PCR for Wnt-1 normalized by GAPDH housekeeping gene (C).

neuronal cell differentiation. The decreased gene expression of caspase 3 (-2.30) (an executioner/effector caspase) upon incubation with 1,25D was further confirmed by RT² PCR arrays. Table 1 also shows that several members of the Bcl-2 family of genes, specifically the pro-apoptotic members such as Bax ($+1.18$); BAD ($+1.22$); Bak ($+1.36$) and Bok ($+1.29$), remain unchanged upon 1.25D incubation.

3.5. 1,25D promotes cell cycle arrest in C3H 10T1/2 mesenchymal multipotent cells

The effect of 1,25D (100 nM) on cell cycle components was evaluated at the transcriptional level applying the mouse cell cycle DNA gene array (OMM-020). Table 2 shows the differential cDNA gene expression between the 1,25D-treated and -untreated cells, where the computer-generated ratios of spot intensities, normalized by housekeeping genes are tabulated. DNA microarray analysis shows a general decrease in the gene expression of cyclins such as Cyclin A2 (-2.76), B1 (-2.15), B2 (-2.9), D1 (-2.32), E1 (-4.39), and F (-3.24), and Cyclin-dependent kinases such as Cdk2 (-2.05) and genes related to check points such as Chek1 (checkpoint kinase 1) (-4.7). We also observed a decreased expression of PCNA (proliferating cell nuclear antigen) (-2.05), which is in agreement with the previous data provided by immunocytochemistry (ICC), real-time PCR and western blot; as well as a decreased expression of caspase 3 (-2.05) and Skp2 (S-phase kinase-associated protein 2) (-2.19), a gene that specifically recognizes phosphorylated cyclin-dependent kinase inhibitor 1B (p27) predominantly in S phase. In order to confirm and to expand the DNA microarray data with a more sensitive procedure, we performed real-time PCR arrays using

Table 2

1,25D regulates the transcriptional expression of cell cycle related genes in C3H 10T1/2 multipotent cells. Total RNA from cells treated as in Fig. 2 was subjected to cDNA microarrays by the Oligo GEArray, Cell Cycle gene array, and the ratios between the 1,25D-treated and 1,25D-untreated cells corrected by GAPDH were calculated for the assays performed in duplicates.

Symbol	Description	DNA microarray ratios (4 days)
Ccna2	Cyclin A2	−2.76
Ccnb1	Cyclin B1	−2.15
Ccnb2	Cyclin B2	−2.9
Ccnd1	Cyclin D1	−2.32
Ccne1	Cyclin E1	−4.39
Ccnf	Cyclin F	−3.24
Cdk2	Cyclin-dependent kinase 2	−2.05
Chek1	Checkpoint kinase 1 homolog (S. pombe)	−4.7
Casp3	Caspase 3	−2.05
Skp2	S-phase kinase-associated protein 2 (p45)	−2.19
PCNA	Proliferating cell nuclear antigen	−2.05

the RT² Profiler™ PCR SuperArray set of primers and procedures (PAMM-020). The ratios for triplicate determinations are shown in Table 3 for 4 days after continuous incubation with or without 1,25D (100 nM). The agreement between the ratios obtained by DNA microarrays and RT² PCR arrays is in general adequate and provides a reasonable assessment of up- and down-gene regulation. The results of the RT² PCR arrays provided confirmatory information related to the cell cycle inhibitory effects of 1,25D on multipotent cells. A substantial decrease in the mRNA expression of numerous cyclins such as Cyclin A2 (-4.39), B1 (-4.87) and B2 (-3.44), and D1 (-2.30) which is a positive regulator of G0/G1 cell cycle progression and a well-known promoter of cell proliferation; Cyclin E1 (-3.21); F (-5.40); cyclin-dependent kinases such as Cdk2 (-2.05) and Cdk4 (-2.25) and genes related to cell cycle check points such as Chek1 (checkpoint kinase 1) (-3.0). Incubation of multipotent cells with 1,25D inhibits G1 to S phase progression by downregulating the expression of the F-box protein Skp2 (p45) (-2.19) that induces cell growth inhibition via G1 arrest.

In order to verify the effect of 1,25D not only at the transcriptional but also at the translational level, several of the most important regulators of cell cycle progression were assessed to further confirm our previous results by western blot. Fig. 6A shows the confirmatory result of the decreased expression of Cyclin D1 and Cyclin D3 upon incubation with 1.25D (100 nM). Fig. 6B shows a decreased expression of Cdk2 (cyclin-dependent kinase 2) and Cdk4 (cyclin-dependent kinase 4) upon incubation with 1.25D (100 nM). Fig. 6C shows that the expression of the cell cycle inhibitor p21 was negligible in the untreated C3H 10T1/2 cells, and 1,25D exposure led to much higher levels of p21 but not p27, mak-

Table 3

Confirmation of the effects of 1,25D on the transcriptional expression of cell cycle related genes in C3H 10T1/2 multipotent cells by real-time PCR arrays. Total RNA from cells treated as in Table 2 was subjected to RT-real-time PCR by the RT² Profiler™ PCR Mouse Cell Cycle Array and the ratios between the 1,25D-treated and 1,25D-untreated cells corrected by GAPDH were calculated for the assays performed in triplicates.

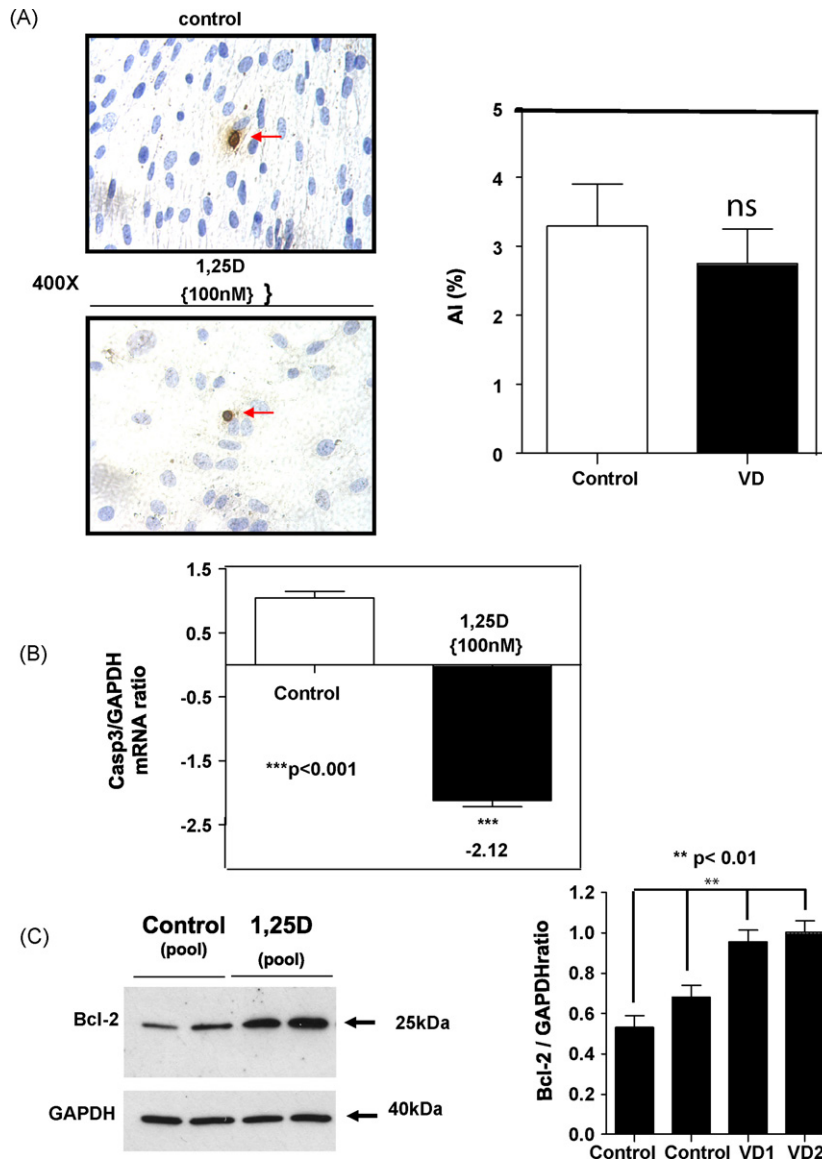| Symbol	Description	Real-time PCR array ratios (4 days)
Ccna2	Cyclin A2	−4.39
Ccnb1	Cyclin B1	−4.87
Ccnb2	Cyclin B2	−3.44
Ccnd1	Cyclin D1	−2.85
Ccne1	Cyclin E1	−3.21
Ccnf	Cyclin F	−4.40
Cdk2	Cyclin-dependent kinase 2	−2.05
Cdk4	Cyclin-dependent kinase 4	−2.25
Chek1	Checkpoint kinase 1 homolog (S. pombe)	−3.0
Skp2	S-phase kinase-associated protein 2 (p45)	−2.60

Fig. 5. 1,25D exerts an anti-apoptotic effect in C3H 10T1/2 multipotent mesenchymal cells. Cells treated as in Fig. 2, were seeded in 8-well chamber slides for TUNEL assay or in 6-well plates for RNA and protein isolation. At the end of the incubation period, samples were subjected to TUNEL assay where the apoptotic index (AI) was obtained for control and VD incubated samples (A). In another set of samples, total RNA isolation was followed by real-time PCR for caspase 3 normalized by GAPDH housekeeping gene. Mean ± SEM corresponds to experiments done in triplicates ***$p < 0.001$. (B) Western blots analysis was performed for extracts from the 4 days incubation time for Bcl-2 normalized with GAPDH with the corresponding densitometric analysis (C).

ing p21 the main primary mediator of the 1,25D anti-proliferative effect in this multipotent cell model.

4. Discussion

Our data demonstrate that the addition of 1,25D to mesenchymal multipotent cells in a time- and dose-dependent manner exerts a potent anti-proliferative effect, inducing cell cycle arrest, promoting the accumulation of cells in G0/G1 phase without inducing apoptosis. This anti-proliferative effect is characterized by a reduction in the number of cells and an increase in cell size compared to the untreated group. Specifically, we demonstrate for the first time, that supplementation with 1,25D decreases cell proliferation and increases cell size through the activation of Rho and Rhou/Wrch-1 pathways without inducing apoptosis. In addition, we demonstrate that 1,25D regulates genes involved in cell cycle progression and key pro-and anti-apoptotic pathways. Supplementation with 1,25D also increases the expression of survivin,

a potentially novel 1,25D-mediated pathway for regulating tissue injury and fibrosis. These advances in our understanding of key mechanistic pathways regulating anti-proliferative and anti-apoptotic effects of 1,25D in a multipotent stem cell model provides an important foundation for future therapeutic interventions such as 1,25D analogs to selected activation of induced pluripotent stem cells in the prevention or treatment of presently considered irreversible hypovitaminosis D related chronic medical conditions such as neoplasias and hyperproliferative disorders including premature organ fibrosis. Although the molecular mechanisms underlying the 1,25D anti-proliferative effect have been widely studied, the molecular mechanisms in many relevant models remain poorly characterized. In this manuscript we first focused on unfolding the inhibitory effect of supplementing mesenchymal multipotent cells with 1,25D by different approaches. These multipotent mesenchymal cells upon incubation with AZCT are able to differentiate into multiple phenotypes, such as contractile striated muscle cells, differentiated adipocytes and chondrocytes [16,17,19,20]. The
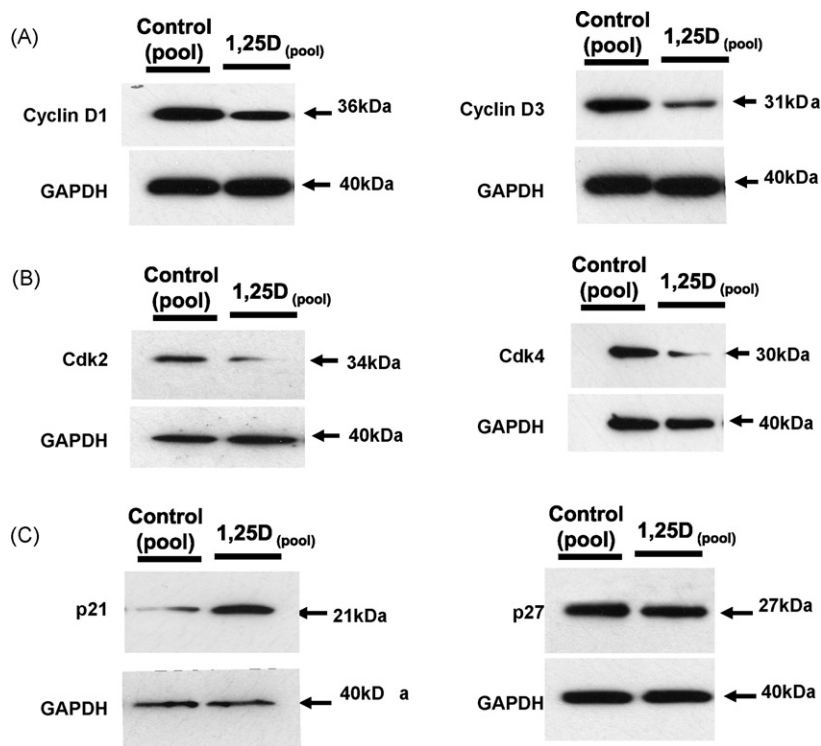
Fig. 6. 1,25D promotes cell cycle arrest in C3H 10T1/2 mesenchymal multipotent cells by decreasing the expression of cyclins, cyclin-dependent kinases (Cdk) and Cdki (cyclin-dependent kinases inhibitors). Cells treated as in Fig. 2, were seeded on 6-well plates for protein isolation Western blots analysis was performed for extracts from the 4 days incubation time for Cyclin D1 and D3 (A), for Cdk2 and Cdk4 (B) and p21 and p27 (C) all of them normalized for housekeeping genes with GAPDH.

number of muscle and fat cells that appear in treated cultures depends on the concentration of 5-azacytidine (20 μM) and the incubation time. Differentiated cells are not observed until 10–15 days after AZCT treatment, when the cells have passed through several division stages [17,19]. In our case, we performed our experiments after 4 days and in same cases after 7 days when the cells were still in a pre-differentiated stage, which allowed us to study the effects of 1,25D on cell proliferation when cells were still in a division stage.

We showed that incubation of multipotent cells in a time- and dose-dependent manner decreases cell proliferation as demonstrated by the decreased expression of PCNA, a protein found in the nucleus that acts as a cofactor of DNA polymerase delta and increases the processivity of leading strand synthesis during DNA replication. The antibody against PCNA recognizes a 36-kDa protein that is present during the S phase [36]; however, in response to DNA damage it is ubiquitinated and is associated in the RAD6-dependent DNA repair pathway, so its detection will mark cell proliferation and DNA repair processes [37]. The data presented in this manuscript also demonstrate that 1,25D decreases cell number and increases cell size, a phenomenon that can be partially attributed to a reduced expression of Rho and Rhou/Wrch-1, but not Wnt-1.

The Rho family of proteins plays a central role in regulating cell shape, polarity and locomotion through their effects on actin polymerization, actomyosin contractility, cell adhesion, and microtubule dynamics [38]. Rho proteins also promote reorganization of the actin cytoskeleton and regulate cell shape, attachment, and motility. It has been shown that overexpression of this gene is associated with tumor cell proliferation and metastasis. Rhou, also known as Wrch-1 (Wnt-regulated Cdc42 homolog) is an atypical member of the Cdc42 subgroup of Rho GTPases. Rhou mRNA level has been shown by Tao et al. to increase in response to Wnt-1 signaling in Wnt-1 transformed mouse mammary epithelial cells [39]. Previous work with fibroblasts and epithelial cells in culture has

shown that Cdc42 contributes to G1 cell cycle progression by promoting entry into G1 and progression to S phase when expressed in quiescent fibroblasts, whereas inhibition blocks serum-induced G1 progression [40]. Moreover, a short hairpin RNA-mediated knockdown of Wrch-1 was shown to perturb cystogenesis in 3D culture, suggesting that tight regulation of Wrch-1 activity is necessary for normal epithelial morphogenesis [41].

Exploring putative mechanisms posited by Eelen et al. [12], we found the addition of 1,25D to mesenchymal multipotent cells blocks the transition from G1 to S phase of the cell cycle accumulating cells in G1 by decreasing the expression of cyclins such as Cyclin A2, B1, B2, D1, D3, E1 and F; as well as cyclin-dependent kinases (Cdk) such as Cdk2 and Cdk4. Of particular interest is that in this multipotent cell model, 1,25D G1/S-blocking effect was accompanied by an increased expression of p21, a Cdk-inhibitor. However, 1,25D does not increase the expression of p27, making p21 a primary candidate for the anti-proliferative effect in C3H 10T1/2 multipotent cells. It is interesting that the stable expression of p27 upon incubation of cells with 1,25D was accompanied by a decreased expression of the F-box protein Skp2 (S-phase kinase-associated protein 2) which, when expressed, positively regulates the G1–S transition by controlling the stability of several G1 regulators, such as the cell cycle inhibitor p27, downregulating Skp2 and as a consequence causing sustained stabilization of p27, which is a key element in the anti-proliferative and anticancer actions of vitamin D.

In this present work, we found the decrease in cell proliferation was not accompanied by an increase in cell apoptosis. On the contrary, addition of 1,25D to the cell cultures exerts an anti-apoptotic effect, characterized by increased expression of the anti-apoptotic protein Bcl-2, a gene that has been thought to promote cell survival in cancer patients [42,43]. Moreover, 1,25D induced a decreased expression of the executioner pro-apoptotic gene caspase 3. These results are in agreement with Zhang et al. [14] who found that

1,25D inhibits hepatocyte apoptosis in rat allografts by regulating apoptotic-associated genes.

Reaffirming the anti-apoptotic effect of 1,25D in our cell model is the fact that the gene expression of Apoptosis inhibitor 5 (Api5/Aac11) increases when the cells have been incubated with 1,25D. Api5/Aac11 is a critical determinant of dE2F1-induced apoptosis *in vivo* and *in vitro*. It has been described that this functional interaction occurs in multiple tissues, and it is conserved from flies to humans. Interestingly, Api5/Aac11 acts downstream of E2F and suppresses E2F-dependent apoptosis without generally blocking E2F-dependent transcription [44].

It is interesting to note that the gene expression of the pro-apoptotic members of the Bcl-2 family such as Bax, Bad, Bak and Bok remains unchanged when the cells have been incubated with 1,25D; reinforcing the anti-apoptotic effect of 1,25D in this multipotent cell model.

We also found an increased expression of survivin, the Baculoviral IAP repeat-containing 5 (Birc5). Survivin contains a baculovirus inhibitor of apoptosis repeat (BIR) a protein domain that is a member of the inhibitor of apoptosis protein (IAP) family. Survivin inhibits apoptosis via its BIR domain, by directly or indirectly interfering with the function of caspases. Survivin is also a chromosomal passenger protein that is required for cell division and is expressed in embryonic tissues as well as in the majority of human cancers, but is not expressed in most normal adult tissues [45]. Recently, emerging evidence suggest that survivin is involved in tissue injury and in wound healing [46,47], which is in agreement with our previous publication regarding the antifibrotic effects of 1,25D in the same multipotent cell system [20].

A previous report by Wei et al. has identified the pro-apoptotic role of activated transcription factor 5 (ATF5) and identified Cyclin D3 as an ATF5-targeted apoptosis-related gene [48]. The same article showed that the ectopic expression of ATF5 in HeLa cells markedly increased cisplatin-induced apoptosis and the cleavage of caspase 3, and induced Cyclin D3 mRNA expression via cooperation with E2F1 transcription factor.

In summary, the addition of 1,25D, the active form of vitamin D, to multipotent mesenchymal cells induced a decrease in cell proliferation, characterized by an increase in cell size, a phenomenon possibly linked to decrease in Rho and Rhou/Wrch-1 expression; it also induced cell cycle arrest, promoting accumulation of cells in G0/G1 phase without inducing apoptosis. The data presented in this manuscript provide a mechanistic explanation for the anti-proliferative and anti-apoptotic properties of 1,25D observed in mesenchymal multipotent cells and provide the mechanistic foundation for not only traditional therapeutic interventions such as 1,25D analogs but also select activation of induced pluripotent stem cells in targeted clinical studies.

Acknowledgements

References

[1] D. Feldman, J.W. Pike, F.H. Glorieux, Vitamin D, 2nd edition, Elsevier Academic Press, 2005 (Chapter 11).

[2] A.S. Dusso, A.J. Brown, Mechanism of vitamin D action and its regulation, Am. J. Kidney Dis. 32 (1998) S13–S24.

[3] A.S. Dusso, A.J. Brown, E. Slatopolsky, Vitamin D, Am. J. Physiol. Renal Physiol. 289 (2005) F8–F28.

[4] D. Zehnder, R. Bland, M.C. Williams, R.W. McNinch, A.J. Howie, P.M. Stewart, M. Hewison, Extrarenal expression of 25-hydroxyvitamin D(3)-1α-hydroxylase, J. Clin. Endocrinol. Metab. 86 (2) (2001) 888–894.

[5] C. Carlberg, M. Quack, M. Herdick, Y. Bury, P. Polly, A. Toell, Central role of VDR conformations for understanding selective actions of vitamin D(3) analogues, Steroids 66 (2001) 213–221.

[6] B.D. Lemon, L.P. Freedman, Selective effects of ligands on vitamin D3 receptor- and retinoid X receptor-mediated gene activation in vivo, Mol. Cell. Biol. 16 (1996) 1006–1016.

[7] C. Rachez, L.P. Freedman, Mechanisms of gene regulation by vitamin D3 receptor: a network of coactivator interactions, Gene 246 (2000) 9–21.

[8] C. Mathieu, R. Bouillon, O. Rutgeerts, M. Vandeputte, M. Waer, Potential role of 1,25(OH)2 vitamin D3 as a dose-reducing agent for cyclosporine and FK 506, Transplant. Proc. 26 (6) (1994) 30–31.

[9] K. Casteels, M. Waer, R. Bouillon, J. Depovere, D. Valckx, J. Laureys, C. Mathieu, 1,25-Dihydroxyvitamin D3 restores sensitivity to cyclophosphamide-induced apoptosis in non-obese diabetic (NOD) mice and protects against diabetes, Clin. Exp. Immunol. 112 (2) (1998) 181–187.

[10] H.H. Malluche, H. Mawad, N.J. Koszewski, Update on vitamin D and its newer analogues: actions and rationale for treatment in chronic renal failure, Kidney Int. 62 (2002) 367–374.

[11] A.S. Dusso, R. Thadhani, E. Slatopolsky, Vitamin D receptor and analogs, Semin. Nephrol. 24 (1) (2004) 10–16.

[12] G. Eelen, C. Gysemans, L. Verlinden, E. Vanoirbeek, P. De Clercq, D. Van Haver, C. Mathieu, R. Bouillon, A. Verstuyf, Mechanism and potential of the growth-inhibitory actions of vitamin D and analogs, Curr. Med. Chem. 14 (17) (2007) 1893–1910.

[13] M. Martinesi, C. Treves, G. d'Albasio, S. Bagnoli, A.G. Bonanomi, M. Stio, Vitamin D derivatives induce apoptosis and downregulate ICAM-1 levels in peripheral blood mononuclear cells of inflammatory bowel disease patients, Inflamm. Bowel Dis. 14 (5) (2008) 597–604.

[14] A. Zhang, Y. Wang, H. Xie, S. Zheng, Calcitriol inhibits hepatocyte apoptosis in rat allograft by regulating apoptosis-associated genes, Int. Immunopharmacol. 7 (8) (2007) 1122–1128.

[15] N. Pendás-Franco, J.M. González-Sancho, Y. Suárez, O. Aguilera, A. Steinmeyer, C. Gamallo, M.T. Berciano, M. Lafarga, A. Muñoz, Vitamin D regulates the phenotype of human breast cancer cells, Differentiation 75 (3) (2007) 193–207.

[16] S. Rainier, A.P. Feinberg, Capture and characterization of 5-aza-2′-deoxycytidine-treated C3H/10T1/2 cells prior to transformation, Proc. Natl. Acad. Sci. U.S.A. 85 (17) (1988 Sep) 6384–6388.

[17] R. Singh, J.N. Artaza, W.E. Taylor, N.F. Gonzalez-Cadavid, S. Bhasin, Androgens stimulate myogenic differentiation and inhibit adipogenesis in C3H 10T1/2 pluripotent cells through an androgen receptor-mediated pathway, Endocrinology 144 (11) (2003) 5081–5088.

[18] M.F. Pittenger, B.J. Martin, Mesenchymal stem cells and their potential as cardiac therapeutics, Circ. Res. 95 (1) (2004) 9–20 (review).

[19] J.N. Artaza, S. Bhasin, T.R. Magee, S. Reisz-Porszasz, R. Shen, N.P. Groome, M.F. Meerasahib, N.F. Gonzalez-Cadavid, Myostatin inhibits myogenesis and promotes adipogenesis in C3H 10T1/2 mesenchymal multipotent cells, Endocrinology 146 (8) (2005) 3547–3557.

[20] J.N. Artaza, K.C. Norris, Vitamin D reduces the expression of collagen and key profibrotic factors by inducing an antifibrotic phenotype in mesenchymal multipotent cells, J. Endocrinol. 200 (2) (2009) 207–221.

[21] I. Fisher, G. Boland, R.S. Tuan, Wnt-3A enhances bone morphogenetic protein-2-mediated chondrogenesis of murine C3H 10T1/2 mesenchymal cells, J. Biol. Chem. 277 (2002) 30870–30878.

[22] E.M. Wilson, P. Rotwein, Control of MyoD function during initiation of muscle differentiation by an autocrine signaling pathway activated by insulin-like growth factor-II, J. Biol. Chem. 281 (40) (2006) 29962–29971.

[23] D. Brackman, J.R. Lillehaug, L. Aksnes, D. Aarskog, Modulation of cell proliferation and cell cycle, and inhibition of cytokinesis by 1,25-dihydroxyvitamin D3 in C3H/10T1/2 fibroblasts, J. Steroid Biochem. Mol. Biol. 46 (2) (1993) 155–162.

[24] J.N. Artaza, R. Singh, M.G. Ferrini, M. Braga, J. Tsao, N.F. Gonzalez-Cadavid, Myostatin promotes a fibrotic phenotypic switch in multipotent C3H 10T1/2 cells without affecting their differentiation into myofibroblasts, J. Endocrinol. 196 (2) (2008) 235–249.

[25] C. Schmittwolf, N. Kirchhof, A. Jauch, M. Durr, F. Harder, M. Zenke, A.M. Muller, In vivo haematopoietic activity is induced in neurosphere cells by chromatin-modifying agents, EMBO J. 24 (2005) 554–566.

[26] S.M. Taylor, P.A. Jones, Multiple new phenotypes induced in 10T1/2 and 2T3 cells treated with azacytidine, Cell 17 (1979) 769–779.

[27] A. Asakura, M. Komaki, M. Rudnicki, Muscle satellite cells are multipotential stem cells that exhibit myogenic, osteogenic, and adipogenic differentiation, Differentiation 68 (2001) 245–253.

[28] R. Jasuja, P. Ramaraj, R.P. Mac, A.B. Singh, T.W. Storer, J. Artaza, A. Miller, R. Singh, W.E. Taylor, M.L. Lee, T. Davidson, I. Sinha-Hikim, N. Gonzalez-Cadavid, S. Bhasin, Delta-4-androstene-3,17-dione binds androgen receptor, promotes myogenesis in vitro, and increases serum testosterone levels, fat-free mass, and muscle strength in hypogonadal men, J. Clin. Endocrinol. Metab. 90 (2) (2005) 855–863.

[29] P. Seale, M.A. Rudnicki, A new look at the origin, function, and stem-cell status of muscle satellite cells, Dev. Biol. 218 (2000) 115–124.

[30] A. Asakura, Stem cells in adult skeletal muscle, Trends Cardiovasc. Med. 13 (2003) 123–128.

[31] B.L. Atkinson, K.S. Fantle, J.J. Benedict, W.E. Huffer, A. Gutierrez-Hartmann, Combination of osteoinductive bone proteins differentiates mesenchymal

C3H/10T1/2 cells specifically to the cartilage lineage, J. Cell. Biochem. 65 (3) (1997) 325–339.

[32] J.N. Artaza, S. Reisz-Porszasz, J.S. Dow, R.A. Kloner, J. Tsao, S. Bhasin, N. Gonzalez-Cadavid, Alterations in myostatin expression are associated with changes in cardiac left ventricular mass but not ejection fraction in the mouse, J. Endocrinol. 194 (1) (2007) 63–76.

[33] J. Essers, A.F. Theil, C. Baldeyron, W.A. van Cappellen, A.B. Houtsmuller, R. Kanaar, W. Vermeulen, Nuclear dynamics of PCNA in DNA replication and repair, Mol. Cell. Biol. 25 (21) (2005) 9350–9359.

[34] P.K. Horan, S.E. Slezak, Stable cell membrane labeling, Nature 340 (6229) (1989) 167–168.

[35] R. Singh, J.N. Artaza, W.E. Taylor, M. Braga, X. Yuan, N.F. Gonzalez-Cadavid, S. Bhasin, Testosterone inhibits adipogenic differentiation in 3T3-L1 cells: nuclear translocation of androgen receptor complex with beta-catenin and T-cell factor 4 may bypass canonical Wnt signaling to down-regulate adipogenic transcription factors, Endocrinology 147 (1) (2006) 141–154.

[36] A. Peled, E. Shezen, D. Schwartz, Y. Shav-Tal, G. Kushtai, B.C. Lee, Y. Gothelf, M. Krupsky, D. Zipori, Nuclear antigen expressed by proliferating cells, Hybridoma 16 (4) (1997) 325–334.

[37] C. Hoege, B. Pfander, G.L. Moldovan, G. Pyrowolakis, S. Jentsch, RAD6-dependent DNA repair is linked to modification of PCNA by ubiquitin and SUMO, Nature 419 (6903) (2002) 135–141.

[38] A.J. Ridley, M.A. Schwartz, K. Burridge, R.A. Firtel, M.H. Ginsberg, G. Borisy, J.T. Parsons, A.R. Horwitz, Cell migration: integrating signals from front to back, Science 302 (2003) 1704–1709.

[39] W. Tao, D. Pennica, L. Xu, R.F. Kalejata, A.J. Levine, Wrch-1, a novel member of the Rho gene family that is regulated by Wnt-1, Genes Dev. 15 (2001) 1796–1807.

[40] M.F. Olson, A. Ashworth, A. Hall, An essential role for Rho, Rac and CDC42 GTPases in cell cycle progression through G1, Science 269 (1995) 1270–1272.

[41] D.C. Brady, J.K. Alan, J.P. Madigan, A.S. Fanning, A.D. Cox, The transforming Rho family GTPase Wrch-1 disrupts epithelial cell tight junctions and epithelial morphogenesis, Mol. Cell. Biol. 29 (4) (2009) 1035–1049.

[42] B. Ilievska Poposka, S. Smickova, S. Jovanovska Crvenkovska, B. Zafirovska Ivanovska, T. Stefanovski, G. Petrusevska, Bcl-2 as a prognostic factor for survival in small-cell lung cancer, Prilozi 29 (2) (2009) 281–294.

[43] A.C. Tsamandas, D. Kardamakis, P. Tsiamalos, A. Liava, V. Tzelepi, V. Vassiliou, T. Petsas, K. Vagenas, V. Zolota, C.D. Scopa, The potential role of Bcl-2 expression, apoptosis and cell proliferation (Ki-67 expression) in cases of gastric carcinoma and correlation with classic prognostic factors and patient outcome, Anticancer Res. 29 (2) (2009) 703–709.

[44] E.J. Morris, W.A. Michaud, J.Y. Ji, N.S. Moon, J.W. Rocco, N.J. Dyson, Functional identification of Api5 as a suppressor of E2F-dependent apoptosis in vivo, PLoS Genet. 172 (11) (2006) 196.

[45] S.K. Chiou, M.K. Jones, A.S. Tarnawski, Survivin — an anti-apoptosis protein: its biological roles and implications for cancer and beyond, Med. Sci. Monit. 9 (4) (2003) 125–129.

[46] M. Zhang, L. Lin, S.J. Lee, L. Mo, J. Cao, E. Ifedigbo, Y. Jin, Deletion of caveolin-1 protects hyperoxia-induced apoptosis via survivin-mediated pathways, Am. J. Physiol. Lung Cell. Mol. Physiol. 297 (5) (2009) L945–L953.

[47] J.Y. Li, X. Gu, H.Z. Yin, Y. Zhou, W.H. Zhang, Y.M. Qin, Protective effect of ischemic preconditioning on hepatic ischemia-reperfusion injury by advancing the expressive phase of survivin in rats, Hepatobiliary Pancreat Dis. Int. 7 (6) (2008) 615–620.

[48] Y. Wei, J. Jiang, M. Sun, X. Chen, H. Wang, J. Gu, ATF5 increases cisplatin-induced apoptosis through up-regulation of cyclin D3 transcription in HeLa cells, Biochem. Biophys. Res. Commun. 13 339 (2) (2006) 591–596.